

# Membranous septum morphology and risk of conduction abnormalities after transcatheter aortic valve implantation

Troels Højsgaard Jørgensen<sup>1\*</sup>, MD, PhD; Nicolaj Hansson<sup>2</sup>, MD, PhD; Ole De Backer<sup>1,3</sup>, MD, PhD; Gintautas Bieliauskas<sup>1</sup>, MD; Christian Juhl Terkelsen<sup>2</sup>, MD, DMSc; Xi Wang<sup>1,4</sup>, MD; Jesper Møller Jensen<sup>2</sup>, MD, PhD; Evald Høj Christiansen<sup>2</sup>, MD, PhD; Nicolo Piazza<sup>5</sup>, MD, PhD; Jesper Hastrup Svendsen<sup>1,3</sup>, MD, DMSc; Bjarne Linde Nørgaard<sup>2</sup>, MD, PhD; Lars Søndergaard<sup>1,3</sup>, MD, DMSc

1. Department of Cardiology, Rigshospitalet, Copenhagen University Hospital, Copenhagen, Denmark; 2. Department of Cardiology, Aarhus University Hospital, Aarhus, Denmark; 3. Department of Clinical Medicine, Faculty of Health and Medical Sciences, University of Copenhagen, Copenhagen, Denmark; 4. Department of Cardiology, West China Hospital, Sichuan University, Chengdu, Sichuan, China; 5. Division of Cardiology, McGill University Health Center, Montreal, ON, Canada; 6. Department of Cardiology and Angiology II, University Heart Center Freiburg - Bad Krozingen, Bad Krozingen, Germany

GUEST EDITOR: Franz-Josef Neumann, MD; Department of Cardiology and Angiology II, University Heart Center Freiburg - Bad Krozingen, Bad Krozingen, Germany

This paper also includes supplementary data published online at: <https://eurointervention.pconline.com/doi/10.4244/EIJ-D-21-00363>

## KEYWORDS

- atrioventricular block
- left bundle branch
- TAVI

## Abstract

**Background:** There are limited data on the association of membranous septum (MS) morphology and transcatheter heart valve (THV) implantation depth, and the development of new conduction abnormalities (CA) after transcatheter aortic valve implantation (TAVI).

**Aims:** The aim of this study was to describe the morphology of the MS and predict the risk of new CA after TAVI based on the MS morphology and THV implantation depth.

**Methods:** Based on preprocedural CT scans, the MS depth was measured for every 25% of the entire MS width in 272 TAVI patients without preprocedural bundle branch block (BBB) or pacemaker. Post-procedural CT scans for THV implantation depth assessment were available in 130 of these patients.

**Results:** The MS depth was a median of 2.5 mm (IQR 1.4-3.8) deeper at the posterior edge when compared to the anterior edge of the MS. New CA developed in 7.1% of patients in whom the THV did not cross the lower MS border at its anterior edge (3.6% with new BBB and high degree CA, respectively), in 18.8% of patients (15.6% with new BBB and 3.1% with new high-degree CA) where the THV overlapped the lower MS border by <2.5 mm and in 47.1% of patients (24.3% with new BBB and 22.9% with new high-degree CA) with THV overlap of the lower MS border by ≥2.5 mm.

**Conclusions:** The difference of the MS depth and THV implantation depth measured at the anterior edge of the MS predicted new CA after TAVI.

\*Corresponding author: Rigshospitalet, The Heart Centre, Blegdamsvej 9, 2100 Copenhagen, Denmark.

E-mail: [troels.hoejsgaard@gmail.com](mailto:troels.hoejsgaard@gmail.com)

## Abbreviations

<b>AV</b>	atrioventricular
<b>CA</b>	conduction abnormalities
<b>CT</b>	computed tomography
<b>L/RBBB</b>	left/right bundle branch block
<b>L/R/NCC</b>	left/right/non-coronary cusp
<b>LVEF</b>	left ventricular ejection fraction
<b>MS</b>	membranous septum
<b>PPM</b>	permanent pacemaker
<b>TAVI</b>	transcatheter aortic valve implantation
<b>THV</b>	transcatheter heart valve

## Introduction

New-onset conduction abnormalities (CA) involving the cardiac conductive tissue from the atrioventricular (AV) node to the bundle branches remain a frequent complication after transcatheter aortic valve implantation (TAVI). The potential clinical impact of CA, such as the need for permanent pacemaker (PPM) implantation, ventricular dysfunction and heart failure, is a particular concern with the expected expansion of TAVI to patients with longer life expectancy<sup>1</sup>.

The membranous interventricular septum (MS) is known to be an anatomical landmark visible by cardiac computed tomography (CT) scan<sup>2-5</sup> functioning as a surrogate for the distance between the native aortic annulus and the AV conduction system<sup>6-9</sup>. The overlap with the lower border of the MS and the inflow portion of the transcatheter heart valve (THV) have been found to predict the risk of PPM implantation after TAVI with good accuracy in previous studies<sup>4,10,11</sup>. The difference of the mean MS depth between patients with and without the need for PPM after TAVI is in the order of 1-2 mm. However, as the lower border of the MS does not run parallel with the native aortic annulus, there is a risk that the MS depth varies within the same patient depending on the location of measurement along the width of the MS. The optimal site of measuring the MS depth and corresponding variation of the THV implantation depth have not been reflected in previous studies.

The aim of this study was to describe the morphology of the MS along the entire width of the MS and evaluate the risk of new-onset CA after TAVI based on the MS depth and THV implantation depth measured by preprocedural and post-procedural CT scans.

## Methods

This retrospective study included all consecutive patients without preprocedural bundle branch block (BBB) or pre-existing PPM treated with TAVI at two Danish sites from 2015 to 2018. Patients with bicuspid aortic valve, previous aortic valve replacement, who died within 30 days after TAVI were excluded. Contrast in the right ventricle is necessary for visualisation of the MS during a CT scan but was not routinely planned due to the retrospective nature of the study. Patients where the MS could not be visualised on the preprocedural CT scan were excluded. Baseline and follow-up data were collected from patient records. Preprocedural and post-procedural electrocardiogram (ECG) data were validated in

all patients. The study was approved by the Danish Data Agency and Danish Patient Safety Authority.

## CONDUCTION ABNORMALITY

A QRS interval  $\geq 120$  ms was defined as BBB and further classified into left (LBBB) or right (RBBB) bundle branch block<sup>12</sup>. High-degree CA (HD-CA) was considered developed if a PPM was implanted due to 2° AV block type 2, 3° AV block or atrial fibrillation with bradycardia, based on class I/II indications for pacing in case of intermittent bradycardia<sup>13</sup>.

Patients were classified into either 1) no CA (absence of BBB on a 12-lead ECG taken closest to 30 days after TAVI and absence of HD-CA diagnosed within 30 days of TAVI), or 2) new CA including patients with 2a) new BBB (new-onset LBBB or RBBB on a 12-lead ECG taken closest to 30 days after TAVI) and 2b) new HD-CA (new-onset HD-CA within 30 days of TAVI regardless of the absence or presence of new BBB).

## CT ACQUISITION

Preprocedural CT scans were performed as part of routine TAVI preparation whereas patients with post-procedural CT scans had been randomly selected due to participation in a previous registry. Scans were performed using local protocols and contemporary single- or dual-source CT scanners with a minimum of 128 detector rows. All scans were ECG-gated with a slice thickness of 0.3-0.8 mm. CT data were analysed using 3mensio Structural Heart 9.1 (Pie Medical Imaging).

## CT ANALYSIS

The analysis of CT data is described in **Figure 1**.

The MS was divided into several points of interest: MS<sub>NCC</sub> – posterior edge of the MS closest to the non-coronary cusp (NCC); MS<sub>RCC</sub> – anterior edge of the MS closest to the right coronary cusp (RCC); MS<sub>25</sub>, MS<sub>50</sub> and MS<sub>75</sub> – at 25%, 50% and 75% of the MS width from the MS<sub>NCC</sub> to the MS<sub>RCC</sub>, respectively; MS<sub>deepest</sub> – at the deepest point of the MS; and MS<sub>CV</sub> – measurements in coronal view.

Based on the preprocedural and post-procedural CT analysis, the difference in THV depth and MS depth was calculated, e.g., at the anterior border of the MS closest to the RCC:  $\Delta\text{THV-MS}_{\text{RCC}} = \text{THV}_{\text{RCC}} \text{ depth} - \text{MS}_{\text{RCC}} \text{ depth}$ . Calcifications of the native aortic leaflets and basal septum were assessed qualitatively and classified as either none, mild, moderate or severe.

## STATISTICAL ANALYSIS

Categorical variables are presented as count and percentage and compared using the chi-squared test. Continuous variables are expressed as mean±standard deviation and compared using the Student's t-test, or median (interquartile range [IQR]) and compared using the Wilcoxon rank-sum test. The risk of new CA in subgroup analysis was calculated with exact binomial confidence limits.

Preprocedural and post-procedural ECG and CT characteristics were investigated as predictors for new CA after TAVI in simple

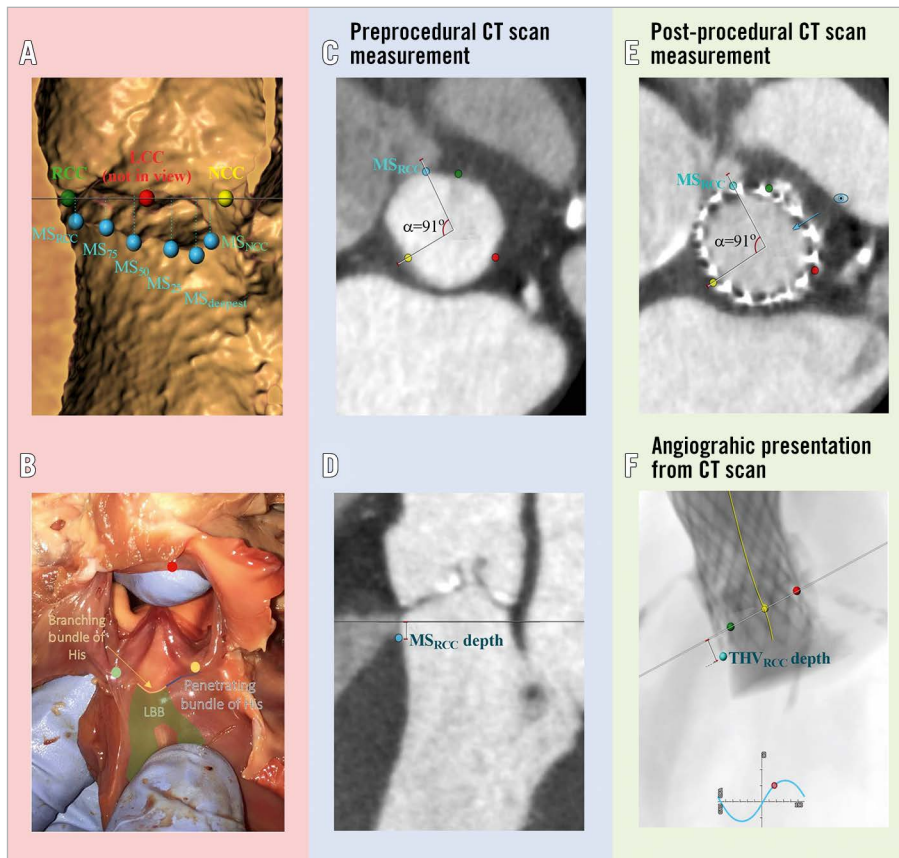


**Figure 1.** Measurement of the membranous septum depth and transcatheter heart valve implantation depth using preprocedural and post-procedural cardiac computed tomography (CT). The native aortic annulus was found as a virtual plane intersecting the nadir of the three native aortic cusps. The MS was visualised both in the aortic annular plane and in an orthogonal plane rotated around the centreline of the aortic annulus. A) & B) The MS (hollow structure in panel A, and pallid structure above the blue and yellow line in panel B) was divided into the different points of interest (blue dots), i.e.,  $MS_{NCC}$  - lower MS border closest to the NCC (yellow dot);  $MS_{RCC}$  - lower MS border closest to the RCC (green dot);  $MS_{25}$ ,  $MS_{50}$  and  $MS_{75}$  - at 25%, 50% and 75% of the MS width from  $MS_{NCC}$  to  $MS_{RCC}$  respectively; and  $MS_{deepest}$  (the MS at its deepest point). MS in coronal view ( $MS_{CV}$ ) is not shown in the Figure. Preprocedural CT analysis: C) Example of marking the location of the  $MS_{RCC}$  in the aortic annular plane. Using the nadir of the NCC and centreline of the aortic annular plane as references the angle to the  $MS_{RCC}$  was registered. D) Measurement of the  $MS_{RCC}$  depth as the distance from the aortic annular plane to the lower MS border at  $MS_{RCC}$ . Post-procedural CT analysis: E) Example of measuring the  $THV_{RCC}$  implantation depth at  $MS_{RCC}$ . The nadir of the native NCC and centreline of the native aortic annular plane on the post-procedural CT scan were again used as references, and the angle to the  $MS_{RCC}$  registered from the preprocedural CT scan was used to mark the point of  $MS_{RCC}$  on the post-procedural CT scan. The CT plane was moved so it would bisect the  $MS_{RCC}$ . Then the C-arm positioning tool of the 3mensio Structural Heart 9.1 (Pie Medical Imaging) software was used, which brings the angiographic projection exactly perpendicular to the positioned plane that bisected the  $MS_{RCC}$  (blue eye and arrow). F) Based on the view from panel E, the THV depth was then measured as the distance from the native aortic annular plane to the inflow edge of the THV lying on top of the MS point of interest ( $THV_{RCC}$  depth in this example). The process of C to E was repeated for all points of interest mentioned in panel A ( $THV_{CV}$  depth was not measured). LBB: left bundle branch; LCC: left coronary cusp (red dot); MS: membranous septum; NCC: non-coronary cusp; RCC: right coronary cusp; THV: transcatheter heart valve

logistic regression analysis. The MS depth was shortest and the THV implantation depth were greatest at the anterior edge of the MS, hence measurements at the  $MS_{RCC}$  was chosen for further investigation. Odds ratio (OR) and area under the operating characteristic curve (AUC) from multiple logistic regression analysis were reported. For multiple logistic regression analysis, the set of

predictor variables included for new CA was prosthesis type and  $MS_{RCC}$  or  $\Delta THV-MS_{RCC}$ . Interobserver variability was tested in 15 patients based on measurements of  $\Delta THV-MS$  along the entire width of the MS. The level of statistical significance was set at 5%. All statistical analyses were performed using SAS Enterprise Guide, version 7.15 (SAS Institute, Inc.).

## Results

New CA developed in 95 of 272 patients (34.9%; 61 patients [22.4%] with new BBB and 34 patients [12.5%] with new HD-CA) (**Figure 2**). Baseline characteristics showed no differences between patients without and with new CA, except for the type of THV implanted and more patients developing CA being in NYHA Class III-IV (**Table 1**). Baseline characteristics of patients with new BBB compared to patients with new HD-CA are shown in **Supplementary Table 1**. The median time to PPM implantation in patients with new HD-CA was 7 days (IQR: 4-8 days). In 16 out of 29 patients who had a PPM implanted, a pacing percentage was available at a median of 167 days (IQR 42-305 days) after the TAVI procedure with a ventricular pacing percentage of 46.5% (IQR 1.8-91.5%). All had a back-up rate of 60 beats per minute. The median time from TAVI to the last available 12-lead ECG used for patient classification was 25 days (IQR: 3-33 days).

### MEMBRANOUS SEPTUM MORPHOLOGY AND THV IMPLANTATION DEPTH

The lower MS border was most frequently deepest at the posterior edge of the MS closest to the NCC (i.e., at the  $MS_{NCC}$ ) and was a median of 2.5 mm (IQR 1.4-3.8) deeper at the  $MS_{NCC}$  when compared to the  $MS_{RCC}$  (**Figure 3A**). On the other hand, the inflow portion of the THV was most frequently implanted deepest at the anterior edge of the MS closest to the RCC (i.e., at the  $MS_{RCC}$ ) and was a median of 0.5 mm (IQR 0.0-1.1) deeper at the  $MS_{RCC}$  when compared to the  $MS_{NCC}$  (**Figure 3B**). The overlap of the THV with the lower MS border was most frequently greatest at the anterior

edge of the MS closest to the RCC (i.e.,  $\Delta THV-MS_{RCC}$ ) and was a median of 3.2 mm (IQR 1.8-4.8) greater compared to the posterior edge of the MS closest to the NCC (i.e.,  $\Delta THV-MS_{NCC}$ ) (**Figure 3**).

The median MS width was similar between the two groups. Patients with new CA had a significantly shorter MS depth and greater THV implantation depth for all points of interest (i.e.,  $MS_{NCC}$ ,  $MS_{25}$ ,  $MS_{50}$ ,  $MS_{75}$ ,  $MS_{RCC}$ ,  $MS_{deepest}$ ,  $MS_{CV}$ ) when compared to patients without CA (**Figure 3A, Figure 3B**).

The median  $\Delta THV-MS$  was greater in patients with new CA at all points of interest when compared to patients without new CA (**Figure 3C**).

### LOGISTIC REGRESSION ANALYSIS OF PREDICTOR FOR NEW-ONSET CONDUCTION ABNORMALITY

In simple logistic regression analysis, the odds for new CA increased significantly with shorter MS depth, greater THV implantation depth and greater  $\Delta THV-MS$  at all of points of interest except for  $MS_{CV}$  depth (**Supplementary Table 2**).

A multiple logistic regression model of preprocedural characteristics showed that the odds of new CA increased significantly with shorter  $MS_{RCC}$  depth (OR 0.82, 95% CI: 0.71-0.93;  $p=0.003$ ) with an AUC of 66% (95% CI: 59-73%); for post-procedural characteristics the odds increased with greater  $THV_{RCC}$  implantation depth (OR 1.71, 95% CI: 1.42-2.16;  $p<0.0001$ ; AUC 82%; 95% CI: 75-90%), and for preprocedural and post-procedural characteristics the odds for new CA increased with greater  $\Delta THV-MS_{RCC}$  (OR 1.49, 95% CI: 1.28-1.79;  $p<0.0001$ ; AUC of 81%; 95% CI: 73-89%) (**Table 2**).

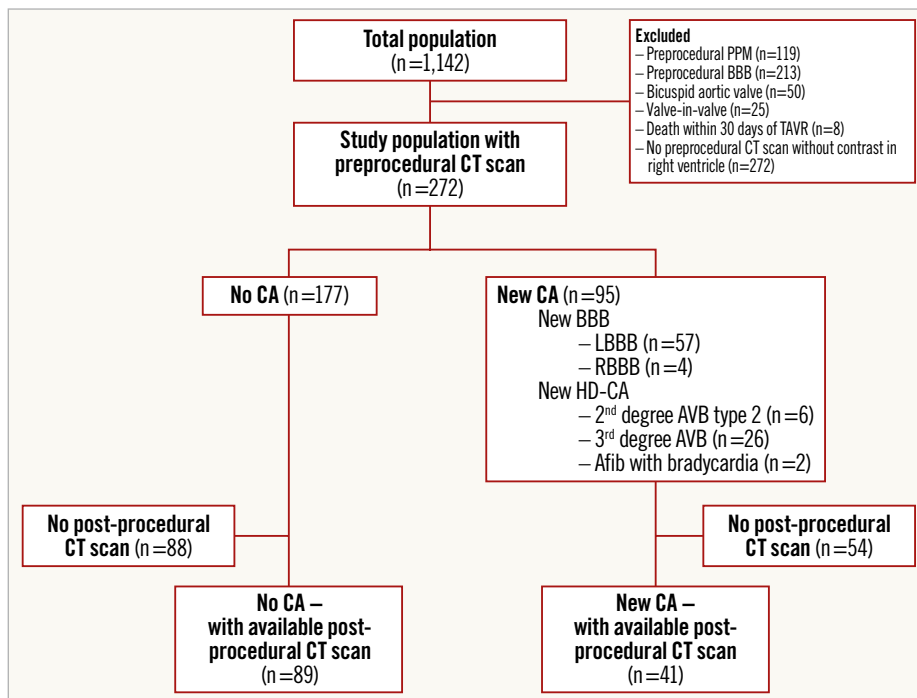


**Figure 2.** Study population. AVB: atrioventricular block; BBB: bundle branch block; CA: conduction abnormalities; CT: computed tomography; HD-CA: high-degree conduction abnormalities; PPM: permanent pacemaker; TAVI: transcatheter aortic valve implantation

**Table 1. Baseline and procedural characteristics.**

	Total (n=272)	No CA (n=177)	New CA (n=95)	p-value	
<b>Baseline</b>					
Age, years	80 (76-85)	81 (76-86)	80 (77-83)	0.22	
Male	129 (46.3)	85 (48.0)	44 (46.3)	0.79	
Diabetes	51/258 (19.8)	31/165 (18.8)	20/93 (21.6)	0.60	
Previous infarction	24 (8.8)	16 (9.0)	8 (8.4)	0.86	
COPD	45 (16.5)	27 (15.3)	18 (19.0)	0.49	
Known atrial fibrillation	79 (29.0)	54 (30.5)	25 (26.3)	0.47	
Dialysis	4/271 (1.5)	1 (0.6)	3/94 (3.2)	0.09	
Previous stroke	33 (12.1)	22 (12.4)	11 (11.6)	1.0	
NYHA Class III-IV	174 (64.0)	123 (69.5)	51 (53.7)	0.01	
STS score, %	2.7 (1.7-3.8)	2.8 (1.8-3.8)	2.6 (1.7-3.5)	0.48	
Preprocedural LVEF, %	60 (50-60)	60 (50-60)	60 (50-60)	0.86	
Preprocedural ECG	PR interval, ms	174 (154-194)	174 (154-193)	174 (155-194)	0.70
	1 <sup>st</sup> degree AVB	39 (14.3)	25 (14.1)	14 (14.7)	0.98
	QRS interval, ms	92 (84-102)	92 (84-100)	94 (84-104)	0.39
<b>Procedural</b>					
Femoral access	244 (89.7)	154 (87.0)	90 (94.7)	0.05	
Prosthesis type – row%	Balloon-expandable	101	76 (75.3)	25 (24.8)	0.002
	Self-expanding	158	97 (61.4)	61 (38.6)	
	Mechanically expandable	13	4 (30.8)	9 (69.2)	
Post-dilation	66 (24.3)	45 (25.4)	21 (22.1)	0.54	
Prosthesis size, mm	27 (26-29)	27 (26-29)	27 (26-29)	0.13	
Oversizing, %	112 (104-118)	108 (103-118)	113 (106-118)	0.08	
Values are median (IQR) or n (%). AVB: atrioventricular block; CA: conduction abnormality; COPD: chronic obstructive pulmonary disease; LVEF: left ventricular ejection fraction; NYHA: New York Heart Association; STS: Society of Thoracic Surgeons					

Interobserver measurement had a paired difference for ΔTHV-MS of -0.7 mm (95% CI: -1.3 mm to -0.08 mm; p=0.03).

**RISK OF NEW-ONSET CONDUCTION ABNORMALITY**

The risk of new CA was evaluated in intervals of 2.5 mm for ΔTHV-MS<sub>RCC</sub>. The risk of new CA increased with greater ΔTHV-MS<sub>RCC</sub>

(p=0.0001) (**Central illustration**). In 28 of 130 patients (21.5%), the THV did not cross the lower MS border at the point of the MS<sub>RCC</sub> (i.e., ΔTHV-MS<sub>RCC</sub> <0 mm) and 2 of these developed new CA (7.1%, 95% CI: 0-16.7, 1 with new BBB and 1 with new HD-CA [3.6%, 95% CI: 0-10.5]). New CA developed in 6 of 32 patients (18.8%, 95% CI: 5.2-32.3; new BBB in 5 patients

**Table 2. Multiple logistic regression of predictors for new-onset conduction abnormality.**

	Preprocedural		Post-procedural		Preprocedural and post-procedural	
	OR (95% CI)	p-value	OR (95% CI)	p-value	OR (95% CI)	p-value
Depth of MS <sub>RCC</sub> – mm	0.82 (0.71-0.93)	0.003	–	–	–	–
THV <sub>RCC</sub> depth – mm	–	–	1.71 (1.42-2.16)	<0.0001	–	–
ΔTHV-MS <sub>RCC</sub> – mm	–	–	–	–	1.49 (1.28-1.79)	<0.0001
Prosthesis type	Balloon-expandable vs self-expanding	0.005	0.75 (0.30-1.89)	0.14	0.85 (0.35-2.13)	0.17
	Mechanically expandable vs self-expanding		4.11 (1.24-16.2)		6.73 (0.73-67.6)	
AUC (95% CI)	0.66 (0.59-0.73)		0.82 (0.75-0.90)		0.81 (0.73-0.89)	
MS <sub>RCC</sub> depth and the difference between the THV <sub>RCC</sub> depth and MS <sub>RCC</sub> depth (ΔTHV-MS <sub>RCC</sub> ) measured at the anterior edge of the lower MS closest to the RCC. Preprocedural versus post-procedural model: p-value=0.0003. Preprocedural versus preprocedural and post-procedural model: p-value <0.0001. Post-procedural model versus preprocedural and post-procedural model: p-value=0.65. AUC: area under the receiver operating characteristic curve; CI: confidence interval; MS: membranous septum; OR: odds ratio; RCC: right coronary cusp; THV: transcatheter heart valve						

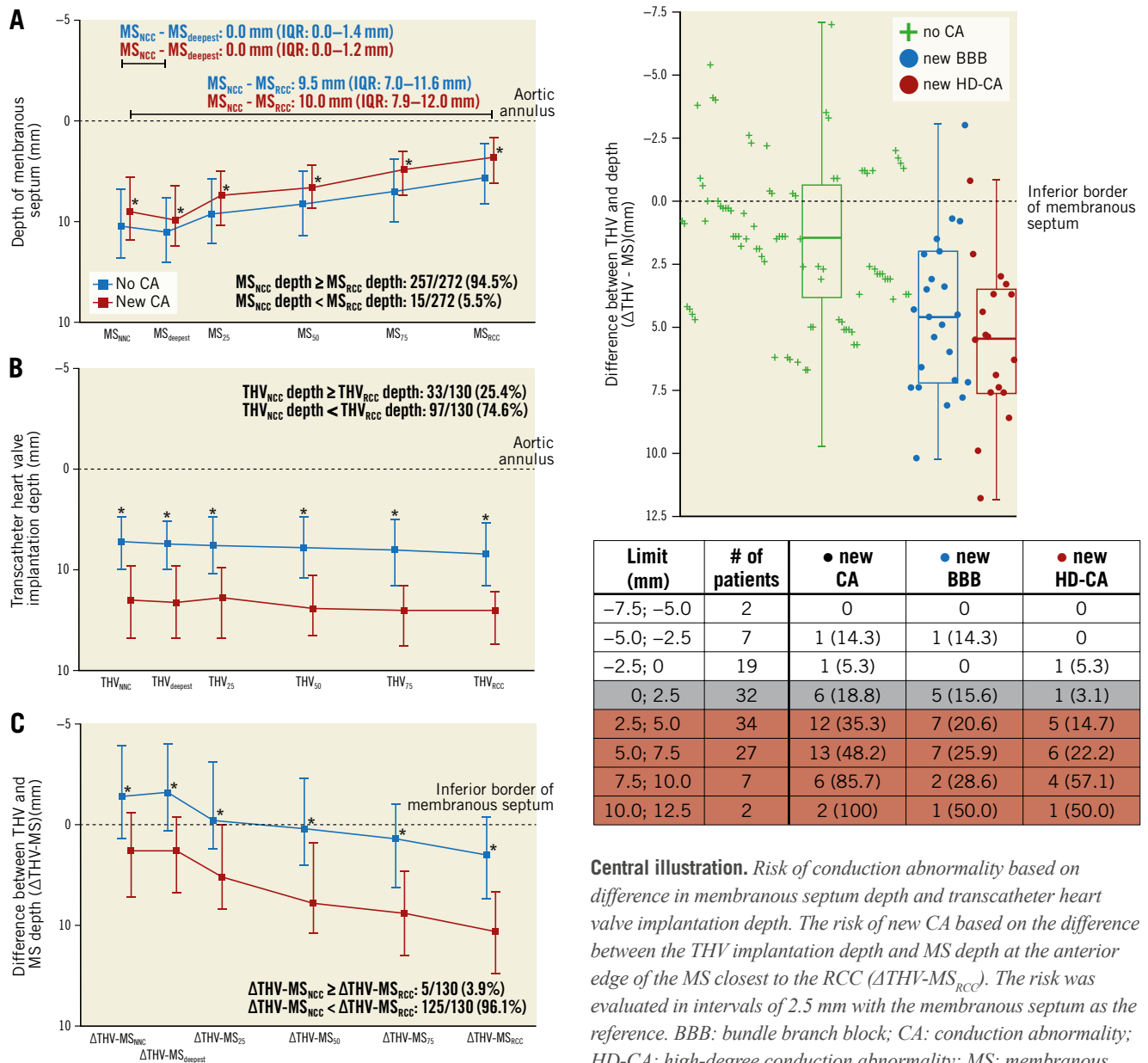


**Figure 3.** Dimensions of the membranous septum and transcatheter implantation depth for patients with or without conduction abnormality. Median and interquartile range shown. A) The MS depth measured at the posterior ( $MS_{NCC}$  depth) and anterior ( $MS_{RCC}$  depth) edges of the lower MS border, at 25% ( $MS_{25}$  depth), 50% ( $MS_{50}$  depth) and 75% ( $MS_{75}$  depth) of the MS width and at the deepest point ( $MS_{deepest}$  depth). B) THV depth measured at the same points of interest as in panel A. C) The difference in MS depth and THV depth ( $\Delta THV-MS=THV$  depth- $MS$  depth) calculated for the same points of interest as in panel A. \* $p<0.05$  for comparison between patients with and without new CA at each point of interest. CA: conduction abnormality; MS: membranous septum; NCC: non-coronary cusp; RCC: right coronary cusp; THV: transcatheter heart valve

[15.6%, 95% CI: 3.0-28.2] and new HD-CA in 1 patient [3.1%, 95% CI: 0-9.2]) with  $\Delta THV-MS_{RCC}$  ( $\geq 0.0$  mm;  $<2.5$  mm), and in 33 of 70 patients (47.1%, 95% CI: 35.5-58.8%) with  $\Delta THV-MS_{RCC}$

$\geq 2.5$  mm (new BBB in 17 patients [24.3%, 95% CI: 14.2-34.3%] and new HD-CA in 16 patients [22.9%, 95% CI: 13.0-32.7%]).

### TRANSCATHETER HEART VALVE INTERSECTION WITH THE MEMBRANOUS SEPTUM

The location where the THV first intersected the lower border of the MS along its width in the posterior-anterior direction (i.e., from the  $MS_{NCC}$  to the  $MS_{RCC}$ ) is shown in **Supplementary Figure 1**. New CA developed in 34 of 85 patients (40.0%) where the THV first intersected the lower MS border within the first 50% of the MS width from the NCC. In 45 patients, the THV first intersected with the lower MS border after more than 50% of the MS width from the NCC or the THV had no contact with the lower MS border. New CA developed in 7 of these patients

(15.6%); the THV intersected the lower MS border before the  $MS_{RCC}$  in all these events except in one patient who developed new BBB.

## Discussion

The depth of the MS varied depending on the site of measuring along the width of the MS and was a median of 2.5 mm shorter at the edge of the MS closest to the RCC when compared to the edge closest to the NCC. MS depth was shorter and the THV implantation depth and  $\Delta THV-MS$  were greater along the entire width of the MS for patients with new CA as compared to patients who did not develop CA. With greater overlap of the  $THV_{RCC}$  and the lower border of the  $MS_{RCC}$  the risk of new BBB and successively new HD-CA increased progressively.

## VARIATIONS OF THE MEMBRANOUS SEPTUM

In accordance with previous studies, the depth of the lower MS border had a large variation between patients<sup>3,5</sup>, but was also found to vary along the MS width within the same patient. This should be considered, as the AV conduction system has been described as being located at the lower border of the MS along its entire width<sup>6-9</sup>. The penetrating part of the bundle of His emerges at the posterior edge of the lower border of the MS closest to the NCC (median  $MS_{NCC}$  depth=4.8 mm in the current study) and continues as the branching part of the bundle of His after one half of the lower MS border (median  $MS_{50}$  depth=3.7 mm in the current study). The branching portion of the bundle of His gives off the fanned out strands of the left bundle branch as it continues towards the anterior edge of the lower MS border closest to the RCC (median  $MS_{RCC}$  depth=2.0 mm in the current study) (**Figure 1B**)<sup>6-9</sup>.

The aim should be to avoid the need for PPM implantation and it is equally important to avoid the development of new-onset BBB (often LBBB and rarely RBBB) after TAVI, considering the increased risk of all-cause mortality and risk of heart failure hospitalisations associated with the development of LBBB or the need for PPM after TAVI<sup>14</sup>. Using the MS as a surrogate for the distance of the target THV implantation zone and to the AV conduction system, the most conservative depth to measure was at the lower MS border at the anterior edge closest to the RCC (i.e., the  $MS_{RCC}$ ), which in the current study was a median of 2.5 mm shorter than the depth measured at the posterior edge of the MS closest to the NCC (i.e.,  $MS_{NCC}$ ).

The MS depth measured in coronal view has previously been reported to predict the development of new AV block<sup>4</sup>. However, this methodology implies some uncertainty. As the nadirs of the aortic leaflets are not definable in this unformatted plane, there is a risk of including a variable section of the interleaflet triangle above the aortic annulus, which may result in overestimation of the MS depth. Moreover, depending on the aortic root angulation, the MS depth could be measured in an oblique direction not perpendicular to the aortic annulus<sup>2,5</sup> (**Supplementary Figure 2**).

## DEPTH OF AORTIC TRANSCATHETER HEART VALVE IMPLANTATION

The increasing risk of new HD-CA mediated by greater  $\Delta THV-MS_{RCC}$  might be due to the THV interacting with more proximal parts of the AV conduction system. Further, it has been reported that greater  $\Delta THV-MS$  was correlated to a greater contact pressure over the lower MS border, which was associated with the development of new CA after TAVI<sup>5</sup>. The AV conduction system is often only covered by a thin layer of endocardium at the lower MS border, but is also found to run several millimetres within the muscular septum in 12.5-32.4% of patients<sup>7,9</sup>. The padding of muscular septum might explain why some patients with a  $\Delta THV-MS_{RCC} \geq 0.0$  mm do not develop CA after TAVI. Conversely, in some cases the bundle of His has been found to be contained totally within the inferior border of the MS, locating the origin of the LBB more anteriorly than usual<sup>8,9</sup>, potentially causing some patients to be at risk of new HD-CA even though  $\Delta THV-MS_{RCC}$  is  $< 0$  mm.

The small extent of the  $MS_{RCC}$  depth might limit the usage of measuring the MS depth in a clinical setting, as the THV implantation depth can be difficult to control within a few millimetres. Likewise, the abovementioned factors might result in too great complexity for the MS depth to be used reliably and which is the reason why we found the THV implantation depth to be an equal predictor for the development of CA after TAVI. However, in the MIDAS study the THV implantation depth was reduced from a mean of 3.3 mm in the retrospective group compared to a mean depth of 2.3 mm in the patient population where THV implantation depth was guided by the MS depth and the risk of new CA statistically significantly reduced (9.7% compared with 3.0%)<sup>10</sup>.

## CLINICAL IMPACT

In the current study, the THV implantation depth measured at the edge of the MS closest to the RCC in general gave the most conservative distance between the inflow portion of the THV and the lower border of the MS. However, isolating this part of the MS tends to lead to C-arm angulations and greater tissue thickness, suboptimal for the THV implantation view. Alternatively, bringing the planes of the THV inflow portion and the native aortic annulus parallel would result in the THV implantation depth measured at a single location being equal to all measurements of THV implantation depth along the circumference of the aortic annulus. Using the double S-curve approach for implantation gives the C-arm angulation point where the delivery catheter and the aortic annulus appear perpendicular, but the method is cumbersome without the right software. However, the implantation view obtained with the double S-curve approach has recently been reported to be very similar to the implantation view obtained with the cusp-overlap method where the LCC and RCC are overlapping and the NCC is isolated inferiorly<sup>15</sup>.

Transient new CA after TAVI is common and thought to be due to inflammation and oedema in the tissue of the AV conduction system and often resolves within 30 days. In a recent study,

multiple regression analysis including preprocedural and post-procedural characteristics showed that  $\Delta$ THV-MS  $\geq 3$  mm and LCC calcification predicted the development of persistent pacing dependency 30 days after TAVI in patients with PPM implantation after TAVI<sup>11</sup>. The increased risk of persistent CA in some patients after TAVI with greater overlap of the MS and lower inflow part of the THV is probably due to the struts of the THV crushing and causing permanent damage to the AV conduction system.

With an increased risk of heart failure and death in patients with BBB or the need for right ventricular pacing<sup>14</sup>, the development of new CA after TAVI is particularly problematic as the indication for TAVI moves to patients with longer life expectancy<sup>16</sup>. Perhaps patients with a high risk of persistent pacing dependency and long life expectancy might benefit from cardiac resynchronisation therapy or bundle of His pacing, while patients with a transient need for a PPM could benefit from a lowered back-up rate so as to promote intrinsic conduction. However, the optimal follow-up therapy for patients with new CA after TAVI is still unknown. Whether measuring the THV implantation depth based on the cusp-overlap method, with or without the MS<sub>RCC</sub> depth as a guide, would result in a higher rate of THV repositioning and lower rate of new CA needs to be confirmed in future studies.

## Limitations

Multiple types of THV were included in the study. The various THVs might exert different radial force at their ventricular part, which is known to be associated with the development of new CA<sup>5</sup>. There is a possibility that the preprocedural and post-procedural CT scans were not perfectly lined up, as alignment was dependent on several measurements. Further, the high exclusion rate and the retrospective nature of the study may have led to bias.

## Conclusions

The MS is a small and irregular structure. The depth of the MS varied between patients and also within the same patient depending on the site of measuring along the width of the MS and was shortest at the edge of the MS closest to the RCC. The difference between THV<sub>RCC</sub> depth and MS<sub>RCC</sub> depth at the edge of the MS closest to the RCC ( $\Delta$ THV-MS<sub>RCC</sub>) predicted the development of new BBB and successively new HD-CA after TAVI. Future studies should investigate the clinical impact of using the MS<sub>RCC</sub> depth as a patient-specific lower limit for THV implantation depth.

## Impact on daily practice

The depth of the MS varies significantly within the same patient depending on the site of measurement along the width of the MS. This should be taken into consideration both in a scientific and in a clinical setting when using MS depth as a predictor for the development of new BBB or HD-CA after TAVI. Further, with greater overlap of the THV and the lower border of the MS, the risk of new BBB and new HD-CA increased progressively.

## Guest Editor

This paper was guest edited by Franz-Josef Neumann, MD; Department of Cardiology and Angiology II, University Heart Center Freiburg - Bad Krozingen, Bad Krozingen, Germany.

## Conflict of interest statement

T.H. Jørgensen has received a research grant from Edwards Lifesciences. L. Søndergaard has received consultant fees and institutional research grants from Abbott, Boston Scientific, Edwards Lifesciences, Medtronic and Symetis. J.H. Svendsen is on the advisory board of Medtronic, has received speaker fees from Medtronic and Biotronik, and has received institutional research grants from Medtronic, Biotronik and Gilead. N. Piazza is a consultant to Medtronic, Peijia and MicroPort. O. De Backer has received institutional research grants and consulting fees from Abbott and Boston Scientific. The Guest Editor reports lecture fees paid to his institution from Amgen, Bayer Healthcare, Biotronik, Boehringer Ingelheim, Boston Scientific, Daiichi Sankyo, Edwards Lifesciences, Ferrer, Pfizer and Novartis, consultancy fees paid to his institution from Boehringer Ingelheim, and grant support from Bayer Healthcare, Boston Scientific, Biotronik, Edwards Lifesciences, GlaxoSmithKline, Medtronic and Pfizer. The other authors have no conflicts of interest to declare.

## References

- Auffret V, Puri R, Urena M, Chamandi C, Rodriguez-Gabella T, Philippon F, Rodés-Cabau J. Conduction Disturbances After Transcatheter Aortic Valve Replacement: Current Status and Future Perspectives. *Circulation*. 2017;136:1049-69.
- Tretter JT, Mori S, Saremi F, Chikkabyrappa S, Thomas K, Bu F, Loomba RS, Alsaied T, Spicer DE, Anderson RH. Variations in rotation of the aortic root and membranous septum with implications for transcatheter valve implantation. *Heart*. 2018;104:999-1005.
- Mori S, Tretter JT, Toba T, Izawa Y, Tahara N, Nishii T, Shimoyama S, Tanaka H, Shinke T, Hirata KI, Spicer DE, Saremi F, Anderson RH. Relationship between the membranous septum and the virtual basal ring of the aortic root in candidates for transcatheter implantation of the aortic valve. *Clin Anat*. 2018;31:525-34.
- Hamdan A, Guetta V, Klempfner R, Konen E, Raanani E, Glikson M, Goitein O, Segev A, Barbash I, Fefer P, Spiegelstein D, Goldenberg I, Schwammenthal E. Inverse Relationship Between Membranous Septal Length and the Risk of Atrioventricular Block in Patients Undergoing Transcatheter Aortic Valve Implantation. *JACC Cardiovasc Interv*. 2015;8:1218-28.
- Rocatello G, El Faquir N, De Santis G, Iannaccone F, Bosmans J, De Backer O, Søndergaard L, Segers P, De Beule M, de Jaegere P, Mortier P. Patient-Specific Computer Simulation to Elucidate the Role of Contact Pressure in the Development of New Conduction Abnormalities After Catheter Based Implantation of a Self-Expanding Aortic Valve. *Circ Cardiovasc Interv*. 2018;11:e005344.
- Elizari MV. The normal variants in the left bundle branch system. *J Electrocardiol*. 2017;50:389-99.
- Kawashima T, Sasaki H. A macroscopic anatomical investigation of atrioventricular bundle locational variation relative to the membranous part of the ventricular septum in elderly human hearts. *Surg Radiol Anat*. 2005;27:206-13.
- Kawashima T, Sato F. Visualizing anatomical evidences on atrioventricular conduction system for TAVI. *Int J Cardiol*. 2014;174:1-6.
- Massing GK, James TN. Anatomical configuration of the His bundle and bundle branches in the human heart. *Circulation*. 1976;53:609-21.
- Jilaihawi H, Zhao Z, Du R, Staniloae C, Saric M, Neuburger PJ, Querijero M, Vainrib A, Hisamoto K, Ibrahim H, Collins T, Clark E, Pushkar I, Bamira D, Benenstein R, Tariq A, Williams M. Minimizing Permanent Pacemaker Following Repositionable Self-Expanding Transcatheter Aortic Valve Replacement. *JACC Cardiovasc Interv*. 2019;12:1796-807.
- Nai Fovino L, Cipriani A, Fabris T, Massussi M, Scotti A, Lorenzoni G, Guerra MC, Cardaioli F, Rodinò G, Matsuda Y, Masiero G, Leoni L, Zorzi A, Fracaro C, Tarantini G. Anatomical Predictors of Pacemaker Dependency After Transcatheter Aortic Valve Replacement. *Circ Arrhythm Electrophysiol*. 2021;14:e009028.



12. Surawicz B, Childers R, Deal BJ, Gettes LS, Bailey JJ, Gorgels A, Hancock EW, Josephson M, Kligfield P, Kors JA, Macfarlane P, Mason JW, Mirvis DM, Okin P, Pahlm O, Rautaharju PM, van Herpen G, Wagner GS, Wellens H; American Heart Association Electrocardiography and Arrhythmias Committee, Council on Clinical Cardiology; American College of Cardiology Foundation; Heart Rhythm Society. AHA/ACCF/HRS Recommendations for the standardization and interpretation of the electrocardiogram: part III: intraventricular conduction disturbances: a scientific statement from the American Heart Association Electrocardiography and Arrhythmias Committee, Council on Clinical Cardiology; the American College of Cardiology Foundation; and the Heart Rhythm Society. Endorsed by the International Society for Computerized Electrocardiology. *J Am Coll Cardiol*. 2009;53:976-81.

13. European Society of Cardiology (ESC); European Heart Rhythm Association (EHRA), Brignole M, Auricchio A, Baron- Esquivias G, Bordachar P, Boriani G, Breithardt OA, Cleland J, Deharo JC, Delgado V, Elliott PM, Gorenek B, Israel CW, Leclercq C, Linde C, Mont L, Padeletti L, Sutton R, Vardas PE. 2013 ESC guidelines on cardiac pacing and cardiac resynchronization therapy: the task force on cardiac pacing and resynchronization therapy of the European Society of Cardiology (ESC). Developed in collaboration with the European Heart Rhythm Association (EHRA). *Europace*. 2013;15:1070-118.

14. Jørgensen TH, De Backer O, Gerds TA, Bieliauskas G, Svendsen JH, Søndergaard L. Mortality and Heart Failure Hospitalization in Patients With Conduction Abnormalities After Transcatheter Aortic Valve Replacement. *JACC Cardiovasc Interv*. 2019;12:52-61.

15. Ben-Shoshan J, Alosaimi H, Lauzier PT, Pighi M, Talmor-Barkan Y, Overtchouk P, Martucci G, Spaziano M, Finkelstein A, Gada H, Piazza N. Double S-Curve Versus Cusp-Overlap Technique: Defining the Optimal Fluoroscopic Projection for TAVR With a Self-Expanding Device. *JACC Cardiovasc Interv*. 2021;14:185-94.

16. Otto CM, Nishimura RA, Bonow RO, Carabello BA, Erwin JP 3rd, Gentile F, Jneid H, Krieger EV, Mack M, McLeod C, O'Gara PT, Rigolin VH, Sundt TM 3rd, Thompson A, Toly C. 2020 ACC/AHA Guideline for the Management of Patients With Valvular Heart Disease: A Report of the American College of Cardiology/American Heart Association Joint Committee on Clinical Practice Guidelines. *Circulation*. 2021;143:e35-71.

## Supplementary data

**Supplementary Table 1.** Baseline and procedural characteristics of patients who developed conduction abnormalities.

**Supplementary Table 2.** Simple logistic regression of predictors for new-onset conduction abnormality.

**Supplementary Figure 1.** Location of the transcatheter heart valve intersection with the lower border of the membranous septum.

**Supplementary Figure 2.** Measurement of the membranous septum depth in coronal view.

The supplementary data are published online at:  
<https://eurointervention.pconline.com/doi/10.4244/EIJ-D-21-00363>



## Supplementary data

**Supplementary Table 1. Baseline and procedural characteristics of patients who developed conduction abnormalities.**

	New BBB (n=61)	New HD-CA (n=34)	<i>p</i> -value
<b>Baseline</b>			
Age, years	80 (76–84)	80 (77–82)	0.81
Male	32 (52.5)	19 (55.9)	0.75
Diabetes	14 (23.0)	6 (18.8)	0.64
Previous infarction	5 (8.2)	2 (8.8)	1.0
COPD	15 (24.6)	3 (8.8)	0.06
Known atrial fibrillation	16 (26.2)	9 (26.5)	0.98
Dialysis	3 (4.9)	0	0.55
Previous stroke	7 (11.5)	4 (11.8)	0.75
NYHA Class III-IV	25 (41.0)	19 (55.9)	0.16
STS score, %	2.6 (1.8–3.9)	2.6 (1.5–3.4)	0.54
Preprocedural LVEF, %	55 (50–60)	60 (53–60)	0.23
Preprocedural ECG			
- PR interval, ms	177 (162–194)	164 (148–193)	0.18
- 1 <sup>st</sup> degree AVB	9 (14.6)	5 (14.7)	0.72
- QRS interval, ms	94 (84–104)	91 (84–102)	0.68
<b>Procedural</b>			
Femoral access	57 (93.4)	33 (97.1)	0.65
Prosthesis type – row%			0.13
- Balloon-expandable	12 (48.0)	13 (52.0)	
- Self-expanding	42 (68.9)	19 (31.2)	
- Mechanically expandable	7 (77.8)	2 (22.2)	
Post-dilation	12 (19.7)	9 (26.5)	0.44

Prosthesis size, mm	27 (26-29)	26.5 (26-29)	0.46
Oversizing, %	115 (108-120)	112 (104-116)	0.062

Values are median (IQR) or n (%).

AVB: atrioventricular block; BBB: bundle branch block; COPD: chronic obstructive pulmonary disease; HD-CA: high-degree conduction abnormality; LVEF: left ventricular ejection fraction; NYHA: New York Heart Association; STS: Society of Thoracic Surgeons

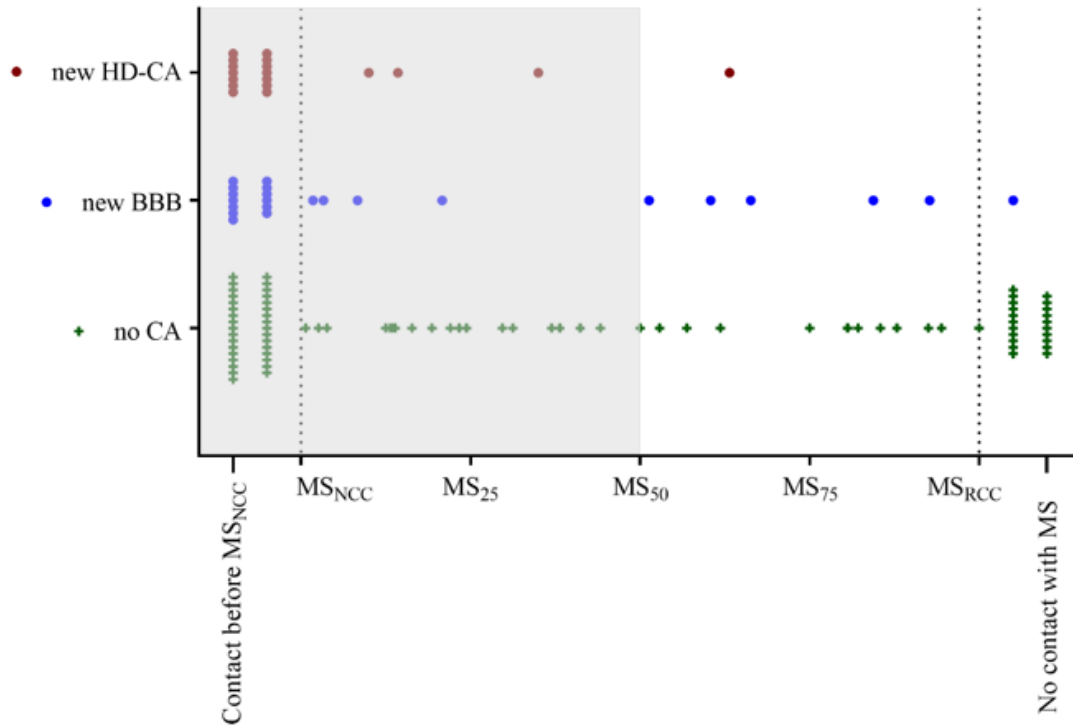
**Supplementary Table 2. Simple logistic regression of predictors for new-onset conduction abnormality.**

	Odds ratio (95% CI)	<i>p</i> -value
<b>MS depth – mm</b>		
- MS <sub>NCC</sub> depth	0.90 (0.80–0.99)	0.041
- MS <sub>25</sub> depth	0.86 (0.76–0.96)	0.011
- MS <sub>50</sub> depth	0.84 (0.74–0.94)	0.004
- MS <sub>75</sub> depth	0.85 (0.75–0.96)	0.008
- MS <sub>RCC</sub> depth	0.82 (0.71–0.93)	0.002
- MS <sub>deepest</sub> depth	0.87 (0.78–0.97)	0.014
- MS <sub>CV</sub> depth	0.99 (0.95–1.02)	0.55
<b>MS width – mm</b>		
	1.01 (0.99–1.02)	0.53
<b>Area of LVOT - cm<sup>2</sup></b>		
	1.08 (0.83–1.42)	0.55
<b>Area of aortic annulus – cm<sup>2</sup></b>		
	1.12 (0.83–1.48)	0.46
<b>Perimeter of aortic annulus/LVOT - %</b>		
	1.04 (0.94–1.15)	0.42
<b>Preprocedural PR interval – ms</b>		
	1.0 (0.99–1.01)	1.0
<b>Preprocedural QRS interval – ms</b>		
	1.01 (0.99–1.03)	0.34
<b>Prosthesis type</b>		
		0.003
- Balloon-expandable vs self-expanding	0.53 (0.30–0.92)	0.026
- Mechanically expandable vs self-expanding	3.64 (1.13–13.9)	0.038
<b>Prosthesis with tapered inflow part</b>		
	1.30 (0.73–2.28)	0.37
<b>Post-dilatation</b>		
	0.84 (0.46–1.51)	0.57
<b>Calcification (moderate/severe vs none/minimal)</b>		
- NCC	0.49 (0.27–0.90)	0.022
- LCC	1.01 (0.61–1.69)	0.98
- RCC	0.70 (0.42–1.17)	0.17
- LVOT	1.34 (0.47–3.62)	0.56
<b>THV depth – mm</b>		
- THV <sub>NCC</sub> depth	1.71 (1.40–2.15)	<0.0001
- THV <sub>25</sub> depth	1.67 (1.38–2.08)	<0.0001
- THV <sub>50</sub> depth	1.72 (1.41–2.15)	<0.0001

- THV <sub>75</sub> depth	1.71 (1.41–2.14)	<0.0001
- THV <sub>RCC</sub> depth	1.67 (1.38–2.08)	<0.0001
- THV <sub>deepest</sub> depth	1.72 (1.41–2.17)	<0.0001
<hr/>		
$\Delta$ THV-MS – mm		
- $\Delta$ THV-MS <sub>NCC</sub>	1.37 (1.19–1.60)	<0.0001
- $\Delta$ THV-MS <sub>25</sub>	1.35 (1.18–1.58)	<0.0001
- $\Delta$ THV-MS <sub>50</sub>	1.46 (1.26–1.73)	<0.0001
- $\Delta$ THV-MS <sub>75</sub>	1.43 (1.24–1.68)	<0.0001
- $\Delta$ THV-MS <sub>RCC</sub>	1.47 (1.27–1.74)	<0.0001
- $\Delta$ THV-MS <sub>deepest</sub>	1.40 (1.22–1.65)	<0.0001

MS depth, THV depth and  $\Delta$ THV-MS=THV depth – MS depth; measured at all points of interest (see **Figure 1**).

LCC: left coronary cusp; LVOT: left ventricular outflow tract (measured 2 mm below the aortic annulus); MS: membranous septum; NCC: non-coronary cusp; RCC: right coronary cusp; THV: transcatheter heart valve

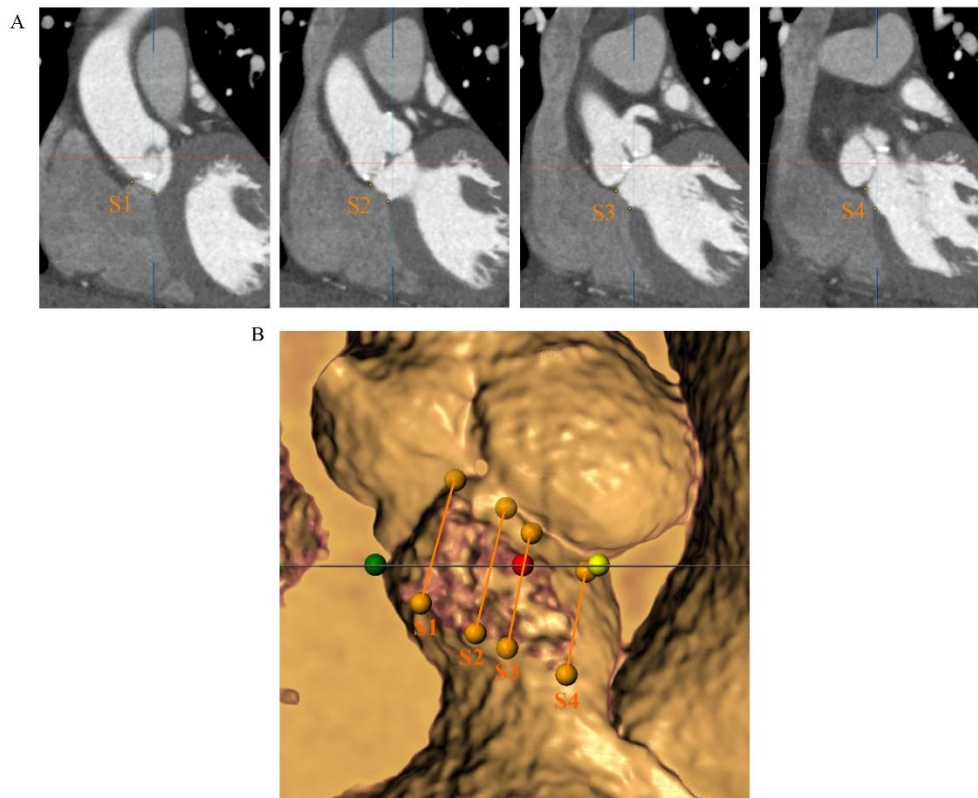


	# of patients	● new-CA	● new BBB	● new HD-CA
Intersection before first 50% of the MS width	85	34 (40.0)	17 (20.0)	17 (20.0)
Intersection after first 50% of the MS width	45	7 (15.6)	6 (13.3)	1 (2.2)

**Supplementary Figure 1.** Location of the transcatheter heart valve intersection with the lower border of the membranous septum.

The location where the THV intersected the lower MS border along its width in the posterior-anterior direction (from MS<sub>NCC</sub> to MS<sub>RCC</sub>).

BBB: bundle branch block; CA: conduction abnormality; HD-CA: high-degree conduction abnormality; MS: membranous septum; THV: transcatheter heart valve



**Supplementary Figure 2.** Measurement of the membranous septum depth in the coronal view.

A) As the nadirs of the aortic cusps are not possible to locate in coronal view, measurements of the MS depth rely on using the hinge points of the cusps.

B) This can result in including a varying segment of the interleaflet triangle depending on which section is used for measuring (e.g., sections 1 to 4 [S1 to S4]) and measuring the MS depth in an oblique direction depending on the angulation of the aortic root.

MS: membranous septum